Springer

Journal of Mechanical Science and Technology 23 (2009) 1132~1141

Journal of Mechanical Science and Technology

www.springerlink.com/content/1738-494x
DOI 10.1007/s12206-008-1214-y

Dynamic analysis of fiber-reinforced elastomeric isolation structures †

Gyung Ju Kang[1] and Beom Soo Kang[2,*]

[1]*School of Mechanical Engineering, Pusan National University, Busan 609-735, Korea*
[2]*Dept. of Aerospace Engineering, Pusan National University, Busan 609-735, Korea*

(Manuscript Received January 28, 2008; Revised December 16, 2008; Accepted December 18, 2008)

Abstract

This paper presents an analysis of seismically isolated buildings using fiber-reinforced elastomeric structures that are subject to excitations caused by earthquakes. In analyzing the vibrations, the buildings are modeled by lumped mass systems. The fundamental equations of motion are derived for base isolated structures, and the hysteretic and nonlinear-elastic characteristics are included in the numerical calculations. The earthquake waves used as the excitation forces are those that have been recorded during strong earthquake motions in order to examine the dynamic stability of building structures. The seismic (nonlinear) responses of the building are compared for each restoring force type and, as a result, it is shown that the building's motions are not so large from a seismic design standpoint. Isolating structures are shown to reduce the responses sufficiently allowing the building's motions to be controlled to within a practical range. By increasing the acceleration of the earthquake, the yielding forces in the concrete and steel frames can be determined, which shows the advantages of performing nonlinear dynamic analysis in such applications.

Keywords: Fiber-reinforced elastomeric isolator (FREI); Steel reinforced elastomeric isolator (SREI); Earthquake; Base isolation; Vibration of building

1. Introduction

Recently, worldwide earthquake induced damage in countries such as Iran, Japan, India, Southeast Asia and North America has been increasing and the damage in low-rise housing properties of 2-3 floors is especially huge. For example, following the incidents in Turkey, Greece, Taiwan, etc. during 1999, low-rise housing buildings suffered casualties of more than 90%. To avoid these damages base isolation methods have been proposed for a long time. The main idea of base isolation is to shift the fundamental frequency of a building structure away from the dominant frequencies found in typical earthquake-induced ground motions. In addition, the aim in adding the isolation systems is to provide energy dissipation mechanisms so that the accelerations transmitted into the building superstructure are reduced. Thus, base isolation systems are designed to essentially decouple the structure from the ground during earthquake excitation.

Current seismic isolation systems of building structures are usually of two types: steel-reinforced multilayer elastomeric systems and mechanisms employing sliding bearings. The rubber bearings form has been used extensively in Japan and South America. The early development of seismic isolation systems using bearings can be backdated to the late 1960s in New Zealand but the concept was considered to be very impractical by most structural engineers in those days. Nowadays, it has become a major strategy for designing earthquake-resistant buildings to protect human lives in United States, Europe and Japan [1-3]. Rubber has been used as the base bearings in the past three decades, following the developments of Kelly [4] in 1976. At present, owing to the tremendous cost of implementing base isolation techniques, applica-

† This paper was recommended for publication in revised form by Associate Editor Dae-Eun Kim

* Corresponding author. Tel.: +82 51 510 2310, Fax.: +82 51 518 4370
E-mail address: bskang@pusan.ac.kr

tions can only be seen in structures with critical or expensive contents. In order to apply seismic isolation for common buildings and public housing, the cost and weight of the isolators need to be drastically reduced. The main reason for the high cost of the isolators is the process used in preparing the steel plates and bonding them to the rubber layers. Also, the high weight of the isolators is due to the same steel plates. Kelly [5] suggested that both the weight and cost of building isolators can be reduced by substituting the steel reinforcing plates with fiber reinforcement of high elastic stiffness. Moon et al. [6] designed and manufactured fiber-reinforced multilayer elastomeric isolators using different kinds of fibers such as carbon, glass, nylon and polyester. From these studies, it was concluded that the performance of carbon fiber-reinforced isolators was even superior to that of the steel-reinforced isolators in view of vertical stiffness, and that they were able to provide effective damping. Kang et al. [7] investigated carbon fiber-reinforced isolator specimens with and without hole and lead plugs. The result of this study was that the hole and lead plugs in fiber -reinforced elastomeric isolators have little effect on improving the effective stiffness and the resulting damping.

Although previous studies have addressed and resolved important aspects, there is a need for assessing the key characteristics influencing the dynamic responses of structures with fiber-reinforced elastomeric isolators. In particular, it is important to examine the dynamic responses of buildings against strong earthquakes when fiber-reinforced elastomeric isolation systems have been added to them. Consequently, it is also necessary to explore specific features of the fibers as reinforcement of the isolator structure. In this paper, the dynamic characteristics of building structures with fiber-reinforced elastomeric isolators under earthquake excitation are examined. After introducing the design procedures of fiber-reinforced elastomeric isolators, the numerical models and dynamic responses needed in this investigations are described.

2. The manufacturing of elastomeric isolator and experiments

The steel-reinforced and fiber-reinforced elastomeric isolators have been fabricated to compare their respective performances. As the stiffness of carbon fiber is higher than that of steel, it has been widely used in fiber-reinforced elastomeric.

2.1 Modelling of steel-reinforced elastomeric isolators

The steel-reinforced elastomeric isolator is composed of layers of rubber and steel plates. The plates protect from lateral bulging of the rubber layers yet allow the rubber layers to undergo shear deformation. The horizontal and the vertical stiffness values are the key performances; the horizontal stiffness (K_H) and vertical stiffness (K_V) of an elastomeric isolator are given as follows:

$$K_H = \frac{GA}{t_r} \tag{1}$$

$$K_V = \frac{E_c A}{t_r} \tag{2}$$

where G is elastic coefficient of rubber; A is the cross-section area of the isolator; t_r is the total thickness of the rubber layers; E_c is the incidental compression stiffness under specific vertical loads in the steel-reinforced isolator. The value of E_c for a single rubber layer is controlled by its shape factor (S) defined as Eq. (3), which is a dimensionless measure of the aspect ratio of the single layer of the elastomeric isolator:

$$S = \frac{loaded\ area}{forced - free\ area}. \tag{3}$$

The shape factor (S) of a circular pad with radius R and thickness t is $S = R/2t$. The model of steel-reinforced elastomeric isolators is shown in Fig. 1.

2.2 Modelling of fiber-reinforced elastomeric isolator

The modelling and design concept for realizing fiber-reinforced elastomeric isolators relies on eliminating the steel reinforcing plates and replacing them with fiber reinforcement of high elastic stiffness, so that the weight and cost of the isolators can be reduced. Fig. 2 shows the model of fiber-reinforced elastomeric isolators. The vertical stiffness of an isolator is the same as Eq. (2), but the effective compression stiffness is given by that shown in Eq. (3), [8]

$$E_c = 6GS^2\left(1 - \frac{6+\nu}{24(1+\nu)}\alpha^2 R^2\right), \quad \alpha^2 = \frac{12(1-\nu^2)G}{E_f t_f t} \tag{4}$$

where, G is the elastic coefficient of rubber; ν is Poisson's ratio; t is the thickness of the rubber layer; E_f is the elastic coefficient of reinforcement; t_f is the thickness of the reinforcement; and S is the shape factor. In the case of rigid reinforcement, the compression stiffness is E_c=6GS. Therefore, with flexible reinforcement, the compression stiffness decreases and accordingly the vertical stiffness also decreases.

2.3 Comparison of nylon FREI and SREI

Some fiber-reinforced elastomeric isolator specimens have been designed and fabricated to compare the characteristics of isolators according to their reinforcing fibers. The dimensions of the specimens are shown in Table 1. In this section nylon is used as the reinforcing fiber. For the sake of comparison, steel-reinforced elastomeric isolator specimens and fiber-reinforced elastomeric isolators with nylon were fabricated and the deformations under vertical load were compared as shown in Fig. 3(a). Under equal vertical loading, the deformation of nylon FREI is higher than that of SREI, which indicates that the vertical loading capacity of nylon FREI is lower than that of SREI. Fig. 3(b) shows the comparison of the horizontal stiffness of SREI and FREI. The tests were carried out using a forcing signal at a frequency of 0.020Hz on each specimen; each test involved the application of a force consisting of four full sine wave cycles. The applied vertical load on the top and bottom plates was 13,000kgf. The rubber layer's thickness was 60.0mm and maximum deformation allowed in the tests was 50% of this rubber thickness. The experimental tests in the fabricated specimens were carried out with a bearing test machine which is capable of subjecting a single bearing to vertical and horizontal loadings simultaneously and is able to develop the maximum axial load of 3,000tonf on the bearing, as shown in Fig. 4. The effective horizontal stiffness, K_{eff} corresponding to each loading cycle, was computed from the secant line, measured from peak-to-peak in each loop.

$$K_{eff} = \frac{F_{\max} - F_{\min}}{D_{\max} - D_{\min}} \tag{5}$$

Here $F_{\max}$ and $F_{\min}$ are the maximum positive and negative shear forces, respectively, and the subscripts, max and min represent the maximum positive and

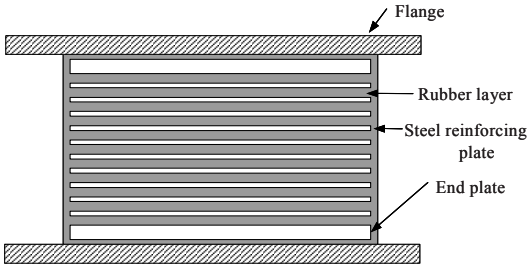

Fig. 1. Model of a steel-reinforced elastomeric isolator (SREI).

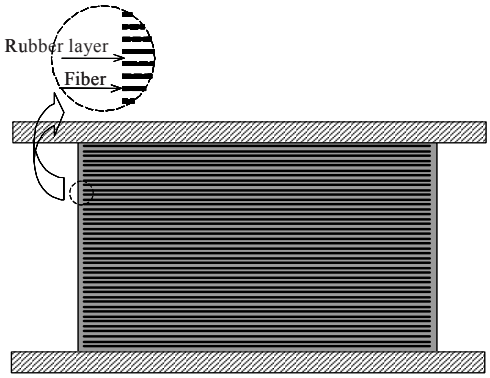

Fig. 2. Model of a fiber-reinforced elastomeric isolator (FREI).

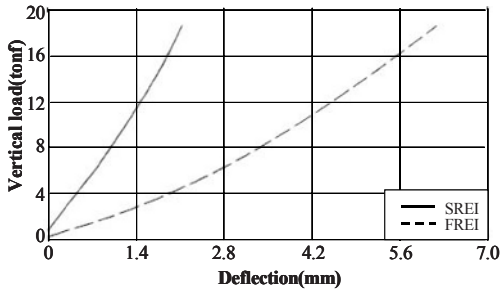

(a) Comparison of vertical tests

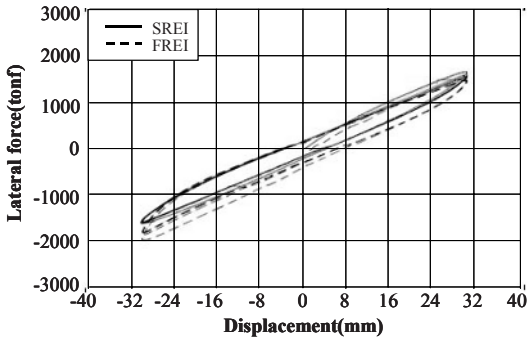

(b) Comparison of horizontal tests

Fig. 3. Comparisons of nylon FREI and SREI.

Table 1. Dimensions of steel- and fiber-reinforced elastomeric isolator bearings.

	Dimension	Isolator section			
		Reinforce-ment	End plate	Inner rubber layer	Total thickness of rubber
SREI	174.5Φ×43 Φ×128T	2T×19EA	15T× 2EA	3T× 20EA	60T
FREI	174.5Φ×43 Φ×128T	1.15T× 75EA	15T× 2EA	0.155T× 76EA	11.75T

Table 2. Test results comparing nylon- and steel-reinforced structures.

Reinforce-ment	Vertical test	Horizontal test		
	Vertical stiffness (kgf/mm)	Tan(ɣ)	Effective stiffness (kgf/mm)	Equivalent Damping(β) (%)
Nylon Fiber	3,550	0.5	26.2	11.16
Steel	9,600	0.5	28.6	6.19

negative shear displacements, respectively. The equivalent viscous damping was computed by measuring the energy dissipated in each cycle (EDC), which is composed of the area that is enclosed by the hysteresis loop. The formula to compute β_{eq} is given as follows [9]:

$$\beta = \frac{EDC}{2\pi K_{eff}\Delta_D^2} D_{\max} \tag{6}$$

where K_{eff} is obtained from Eq. (5), and Δ_D^2 is the average of the positive and negative maximum displacements. K_{eff} and β of SREI under 50% shear deformation are 26.2kgf/mm and 6.19%, respectively. K_{eff} and β of FREI under 50% shear deformation are 28.6kgf/mm and 11.16%, respectively. The test results show that the vertical stiffness of nylon FREI is lower than that of SREI and the damping of nylon FREI is two times higher than that of SREI. The vertical and horizontal test results are shown in Table 2.

2.4 Comparison of carbon FREI and SREI

In the previous section it was shown that the vertical stiffness of nylon-reinforced elastomeric isolators were lower than those of the SREI ones; this results from the fact that the tensional stiffness of nylon is lower than that of steel. The tension stiffness of the nylon can be strengthened by using high carbon fiber, and the seismic characteristics of the new isolator have been investigated. The horizontal and vertical loading tests were carried out on both carbon FREI and SREI samples, and Fig. 5 shows that the vertical stiffness of carbon FREI and SREI under varying vertical loads from 190(tonf) to 370(tonf) were 320,857(kgf/mm) and 107,322(kgf/mm), respectively. The test results indicate that the vertical load of carbon FREI is three times higher than that of SREI. The horizontal and vertical test results are shown in Table 3 and the horizontal test results (see Fig. 6) of Carbon FREI and SREI show that the effective horizontal stiffness and damping of FREI are 330(kgf/mm) and 15.85%, respectively; the effective horizontal stiffness and damping of SREI are 350(kgf/mm) and 6.20%, respectively. These results indicate that the effective damping of carbon FREI is over two-times higher than that of SREI. The vertical test results shows that vertical stiffness of carbon FREI is three-times higher than that of SREI. Because the rubber layers between the fibers are thin, there is little bulging of the rubber and also the tension stiffness of carbon is higher than that of steel plate. It is known that the effective damping of carbon FREI is 2.5 times higher than that of SREI, which means that more earthquake energy can be absorbed using FREI structures.

2.5 Result analysis and dynamic analysis condition

The comparative investigation test results of nylon FREI, carbon FREI and SREI are summarized in Table 4. The results show that for nylon-reinforced structures, both the vertical and horizontal stiffness is decreased, and in case of carbon reinforcement, the stiffness is also increased compared with SREI. Using these test results the dynamic analysis was determined in the vertical and horizontal directions. However, because the horizontal response is the most dominant, our results focus on the horizontal analysis. Eqs. (1) and (2) imply that the horizontal stiffness and the vertical stiffness are independent of the rubber material's property, *G*. Our dynamic analysis was carried out under varying reinforcement stiffness conditions.

3. Theoretical background of dynamic analysis

3.1 Governing equation of motion

The building structure model with fiber-reinforced elastomeric isolator as shown in Fig. 7 consists of a building superstructure and a base isolation structure. The building superstructure has a nonlinear recovering force and the base isolation mechanism was modeled as an elasto-plastic model with spring plus damper characteristics. The shear force of elasto-plastic models against excitations caused by earthquakes between the i^{th} and $i-1^{th}$ floor is $Q_i=K_i(x_i-x_{i-1})+{}_yQ_t$ and has a damping coefficient is C_i, where K_i denotes the elastic stiffness of the i^{th} floor; x and y represent the coordinates. Note that C_i was assigned as a constant damping coefficient. The governing equivalent equation for the i^{th} floor can be obtained as follows:

$$m_i\ddot{x}_i+C_i(\dot{x}_i-\dot{x}_{i-1})+C_{i+1}(\dot{x}_i-\dot{x}_{i+1})+K_i(\dot{x}_i-\dot{x}_{i-1})+K_{i+1}(\dot{x}_i-\dot{x}_{i+1})+{}_yQ_i-{}_yQ_{i+1}=-m_i\ddot{y}_0 \quad (i=1,2,3,\cdots,N) \tag{7}$$

.

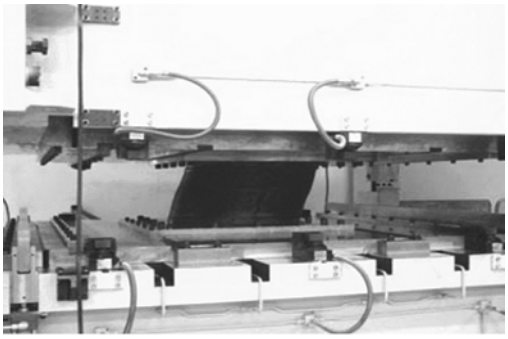

Fig. 4. Test machine in operation.

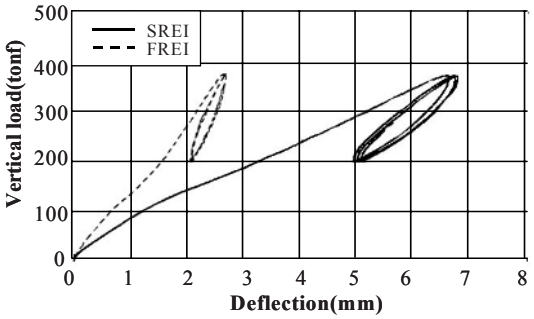

Fig. 5. Comparison of the vertical stiffness of SREI and FREI.

The governing motion equation shown in Eq. (7) can be expressed in matrix form as.

$$M\{\ddot{x}\}+C\{\dot{x}\}+K\{x\}+H\{{}_yQ\}=-ME\{\ddot{y}_0\} \tag{8}$$

where $\{x\}=[x_1 \ \cdots \ x_i \ \cdots \ x_n]^T$,

$\{yQ\}=[{}_yQ_1 \ \cdots \ {}_yQ_i \ \cdots \ {}_yQ_n]^T$, $E=[1 \ \cdots \ 1 \ \cdots \ 1]^T$,

$$H=\begin{bmatrix} 1 & -1 & & & \\ & \ddots & \ddots & & \\ & & 1 & -1 & \\ & & & \ddots & \ddots \\ & & & & 1 \end{bmatrix}, \quad M=\begin{bmatrix} m_0+m_1 & & & \\ & \ddots & & \\ & & m_i & \\ & & & \ddots \\ & & & & m_n \end{bmatrix},$$

$$C=\begin{bmatrix} C_0+C_1+C_2 & -C_2 & & \\ -C_2 & C_2+C_3 & \ddots & \\ & \ddots & \ddots & -C_n \\ & & -C_n & C_n \end{bmatrix}, \quad K=\begin{bmatrix} K_0+K_1+K_2 & -K_2 & & \\ -K_2 & K_2+K_3 & \ddots & \\ & \ddots & \ddots & -K_n \\ & & -K_n & K_n \end{bmatrix}.$$

Table 3. Test results comparing carbon- and steel-reinforcements.

Reinforcement	Vertical test	Horizontal test		
	Vertical stiffness (kgf/mm)	Tan(ɣ)	Effective stiffness (kgf/mm)	Equivalent Damping(β) (%)
Carbon Fiber	320,857	0.5	330	15.85
Steel	107,322	0.5	350	6.20

Table 4. Carbon- and nylon-reinforced elastomeric isolation structures.

		Nylon/steel	Carbon/steel
Vertical test	Vertical stiffness	0.5	3
Horizontal test	Effective stiffness	0.9	0.9
	Damping	2	2

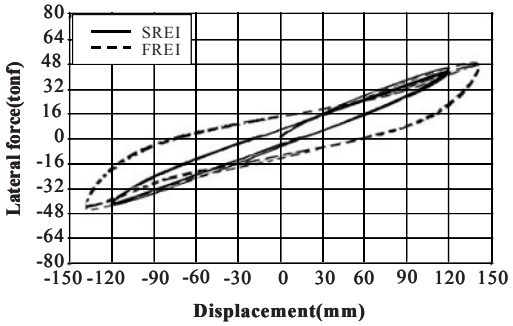

Fig. 6. The hysteresis effect due to the isolators.

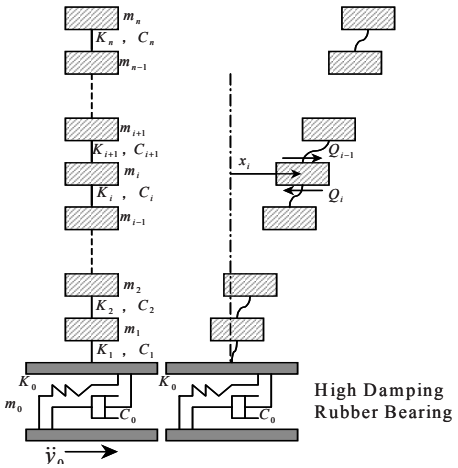

Fig. 7. Elasto-plastic model of a building and isolator.

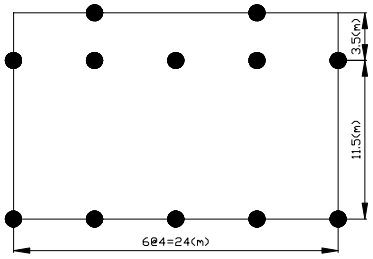

(a)

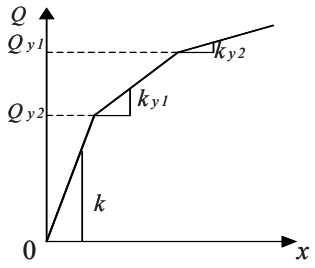

(b)

Fig. 8. Analysis model: (a) Arrangement of FREI; (b) D-trilinear model.

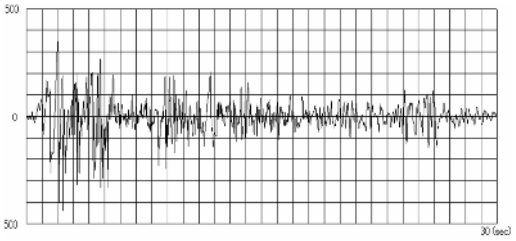

Fig. 9. El-Centro (NS) earthquake wave forces.

3.2 Numerical analysis of the seismic response

The numerical methods used in studying seismically isolated structures will be briefly explained together with the equations of motions that need to be handled. When deformation, velocity and acceleration are independent variables, after expanding the governing motion equation in a Taylor's series, it can be expressed as follows:

$$u_{m+1} = u_m + \tau v_m + \frac{\tau^2}{2} a_m + \frac{\tau^3}{6}\left(\frac{da}{dt}\right)_{t=f} = u_m + \tau v_m + \frac{\tau^2}{2} a(t'),$$
$$v_{m+1} = v_m + \tau a_m + \frac{\tau^2}{2}\left(\frac{da}{dt}\right)_{t=f} = v_m + \tau a(t') \tag{9}$$

where t' and t'' are points of time between the interval(t_m, t_{m+1}) which can be expressed by using superposition of the values of at both ends a_m, a_{m+1}

$$a(t') = (1-2\beta)a_m + 2\beta_{m+1}$$
$$a(t'') = (1-\mu)a_m + \mu a_{m+1} \tag{10}$$

This scheme is the Newmark-β method. In case it is β =1/6, acceleration varies linearly in the section. The value of μ was used as 0.5. With this method, the displacement vector, the velocity and the acceleration were expressed as follows:

$$\{x\} = D,\ \{\dot{x}\} = V/\tau,\ \{\ddot{x}\} = A/\tau^2 \tag{11}$$

From the relation of Eqs. (9) and (10) the following equations are obtained:

$$D_{m+1} = D_m + V_m + \frac{1}{2}[(1-2\beta)A_m + 2\beta A_{m+1}] \tag{12}$$

$$V_{m+1} = V_m + \frac{1}{2}(A_m + A_{m+1}) \tag{13}$$

From Eq. (8) the following equation can be obtained:

$$MA_{m+1}/\tau^2 + CV_{m+1}/\tau + K_{m+1}D_{m+1} + H_y Q_{m+1} = -ME \cdot \ddot{y}_{0_{m+1}} \tag{14}$$

Substituting Eqs. (12) and (13) into Eq. (14), we can obtain:

$$(M/\tau^2+\frac{1}{2}C/\tau+\beta K_{m+1})A_{m+1}+[\frac{1}{2}C/\tau+\frac{(1-2\beta)}{2}K_{m+1}]A_m$$
$$+(C/\tau+K_{m+1})V_m+K_{m+1}D_m+H_yQ_{m+1}=-ME\cdot\ddot{y}_{0_{m+1}} \quad (15)$$

In this paper, the hysteresis characteristics between the interval (t_m, t_{m+1}) were assumed to be constant for convenience in performing the calculations. From Eq. (15) the acceleration at the (m+1) step can be calculated, and from Eqs. (12) and (13) the displacement and velocity can be calculated. From calculated displacement at the (m+1) step, the hysteresis characteristics can be obtained, without repeating the calculation of the results reflected in the next step. Therefore, higher precision calculated results can be obtained by shortening the time interval between the steps.

4. Dynamic analysis of buildings with fiber-reinforced elastomeric isolator

4.1 Modeling of building structure with fiber-reinforced elastomeric isolator

A dynamic analysis was performed of building base isolated structures with 12 isolators which are located on principal frames of low storey building as shown in Fig. 8(a). The recovery force of the building superstructure is shown in Table 5. The building superstructure was assumed to have a D-trilinear recovery characteristic as shown in Fig. 8(b). The damping coefficient of the building and that of the isolator are 0.02 and 0.005, respectively. The yield points of the the D-trilinear Q_{y1}, Q_{y2} relations are selected to allow comparisons with the characteristics of the D-trilinear values arising due to the El-Centro (NS) earthquake wave.

Table 5. Design parameters of a building superstructure.

No.	Weight (tonf)	High (m)	K (tonf/cm)	Qy1 (tonf)	Ky1/k	Qy2 (tonf)	Ky2/k
3	462.4	7.02					
			1902.9	2100.0	0.300	3700.0	0.01
2	449.0	4.09					
			10610.3	3700.0	0.200	7900.0	0.01
1	1029.4	1.24					
Isolator	1940.8		39.99	0.0	1.0	0.0	1.0

4.2 Analysis input data

The seismic response of a multi-storey base-isolated building is investigated under realistic earthquake ground motions. The earthquake motions selected for the study are the NS component of 1940 El-Centro earthquake wave (Fig. 9). The peak ground acceleration (PGA) of the El-Centro earthquake motion is 439 gal(which is a unit of acceleration used extensively in the science of gravimetry and is defined as 1 centimeter per second squared (1 cm/s²)). Fig. 10 shows the acceleration response spectrum caused due to the earthquake, which indicates that there are high acceleration components within 1 second and low acceleration components above 1.5 second. The propagation of the earthquake wave was assumed to be in the longitudinal direction and the analysis was carried out for 30 seconds. The dominant frequency of the earthquake's motions is 3.7-4.5Hz.

4.3 Analysis results

Fig. 11 shows the acceleration responses of each storey of the building isolated by fiber-reinforced elastomeric isolators subjected to the El-Centro, 1940 earthquake's motions. The figure indicates that the

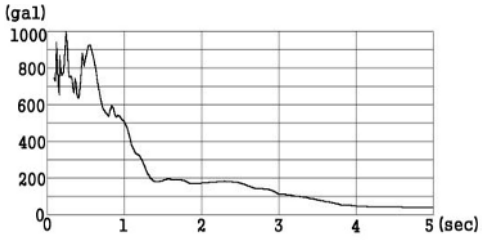

Fig. 10. Building acceleration response spectrum.

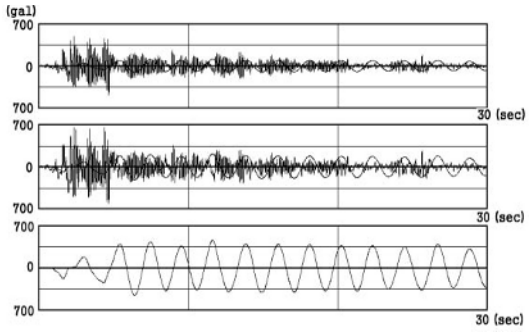

Fig. 11. Time history response of acceleration (1f, 2f, and 3f from bottom graph, respectively).

vibration period with isolator becomes long and the inter-storey deflection decreases, which implies that the fiber-reinforced elastomeric isolator is quite effective for protecting buildings under earthquake excitation. To investigate the dynamic behavior of base-isolated building structures with fiber-reinforced elastomeric isolators, investigations according to the vertical and horizontal stiffness of the isolator, the mode shape responses, the inter-storey absolute acceleration responses and the shear force responses have been carried out. Also, in order to examine the dynamic responses according to acceleration magnitude, the acceleration of the El-Centro (NS) wave was used from half- to two-times magnitude of peak ground acceleration of the El-Centro's data (namely 439gal). The mode shape is plotted in Fig. 12 where it is observed that the second and third order modes are comparatively lower within 5% of the first order mode. The figure indicates that the first mode is clearly dominant and the building superstructure moves without torsion. Fig. 13 shows that the absolute acceleration responses of 1f, 2f, and 3f are almost the same with varying isolator stiffness. The analysis with low stiffness implies that the dynamic analysis for low stiffness isolators such as nylon FREI and also high stiffness ones indicate the case of carbon FREI. It is observed that in low stiffness cases, the absolute acceleration response is comparatively low. The inter-storey shear forces are compared for varying isolator stiffness, and the results are shown in Fig. 14. The figure indicates that the shear forces are high at lower storeys, which means that the possibility of collapse is high for comparatively low storeys. Also, it is observed that at low stiffness values, the shear force is low. Fig. 15 shows the absolute acceleration response for various accelerations, and it is observed that the absolute acceleration increases when high magnitude accelerations are applied.

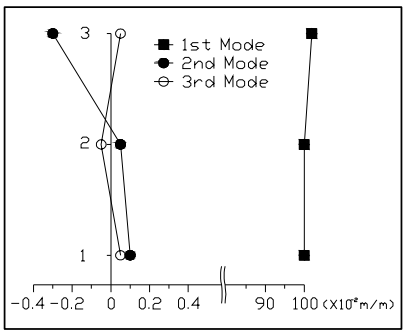

Fig. 12. Mode shape.

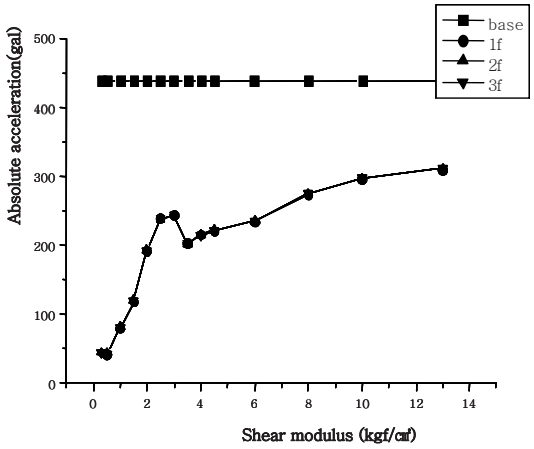

Fig. 13. Absolute time response.

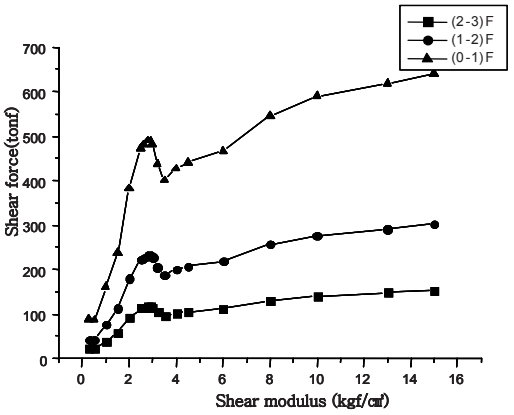

Fig. 14. Shear force response of each storey.

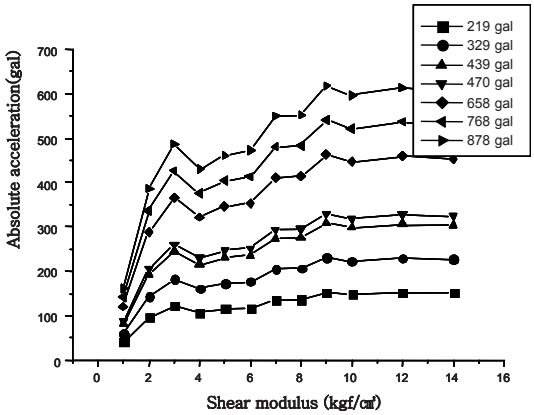

Fig. 15. Responses due to various magnitudes of earthquake.

5. Conclusions

The analytical seismic response of multi-storey buildings isolated by fiber-reinforced elastomeric isolators is investigated under strong earthquake conditions. The recorded earthquake wave El-Centro (NS) is used to investigate the variation of the top floor acceleration and bearing displacement of an isolated building. The response of the isolated building structure is plotted under different magnitudes of earthquakes. From the results obtained, certain trends and conclusions may be drawn. As the frequency of the building structure increases, accordingly the inter-storey deformation decreases. FREI with low stiffness fiber such as nylon shows low acceleration responses, but on the other hand with high stiffness such as obtained using carbon fiber shows high acceleration responses. The motion of the building superstructure with isolator is smoother than that without an isolator. The value of the acceleration responses increases in accordance with the magnitude of the earthquake input. Parametric studies indicate that both inter-storey deformations and floor accelerations increase with the strength of the earthquake. In order to ensure low acceleration responses, comparatively high damping isolators are suggested as potential practical protections mechanisms of building against strong earthquakes. The results reported herein could provide a better understanding to develop more advanced fiber - reinforced elastomeric isolators. Moreover, it is believed that this study can be utilized to provide the dynamic properties of fiber-reinforced elastomeric isolators.

Acknowledgment

This work has been supported by the Korea Science and Engineering Foundation (KOSEF) NRL Program grant funded by the Korea Government (MEST) (No. R0A-2008-000-20017-0). Also the last author would like to acknowledge the partial support by grants-in-aid for the National Core Research Center program from MOST/KOSEF (No. R15-2006-022-02002-0).

References

[1] J. M. Kelly, Seismic isolation of civil buildings in the USA, *Progress in Structural Engineering and Materials*, 1 (3) (1998) 279-285.

[2] A. Martelli and M. Forni, Seismic isolation of civil buildings in Europe, *Progress in Structural Engineering and Materials*, 1 (3) (1998) 286-294.

[3] T. Fujita, Seismic isolation of civil buildings in Japan, *Progress in Structural Engineering and Materials*, 1 (3) (1998) 295-300.

[4] J. M. Kelly, *Earthquake-resistant design with rubber*, Second Ed. Springer, London, U.K., (1997).

[5] J. M. Kelly, Analysis of fiber-reinforced elastomeric isolators. *J. Seismol. Earthquake Eng*., 2 (1) (1999) 19-34.

[6] B. Y. Moon, G. J. Kang, B. S. Kang and J. M. Kelly, Design and manufacturing of fiber reinforced elastomeric isolator for seismic isolation, *J. Mater. Process. Technol*, 130/131 (2002) 145-150.

[7] B. S. Kang, G. J. Kang and B. Y. Moon, Hole and lead plug effect on fiber reinforced elastomeric isolator for seismic isolation, *J. Mater. Process. Technol.*, 140 (2003) 592-597.

[8] J. M. Kelly, Analysis for fiber-reinforced elastomeric isolators. *Annual Report to Engineering Research Center for Net-Shape and Die Manufacturing Pusan National University Korea*. (2000).

[9] B. Y. Moon, G. J. Kang, B. S. Kang and K. S. Kim, Design and experimental analysis of fiber reinforced elastomeric isolator, *Transactions of the KSME, A*., 26 (10) (2002) 2026-2033.

Gyung-Ju Kang received a B.S., M.S. and Ph.D degrees in Aerospace Engineering from Pusan National Univer-sity, Korea, in 1997, 1999 and 2005, respectively. Dr. Kang's re-search interests are in the area of seismic bearing design, base isolation, cold forging, and steel structure.

Beom-Soo Kang received a B.S. degree in Mechanical Engineering from Pusan National University, Busan, Korea in 1981. He then went on to receive his M.S. degree in Aerospace Engineering from KAIST (Korea Advanced Institute of Science and Technology) Seoul, Korea, in 1983 and Ph.D. degree in Mechanical Engineering from University of California at Berkeley in 1990. Dr. Kang is currently a Professor at Department of Aero-space Engineering at Pusan National University. He is currently serving as the Director of ILIC (Industrial Liaison Innovation Cluster). Dr. Kang's re-search interests include flexible forming, unmanned system design, multi-stage deep drawing, and cold forging.